

Rotationally resolved spectra of jet-cooled VMo

Ramya Nagarajan, Shane M. Sickafoose, and Michael D. Morse^{a)}

Department of Chemistry, University of Utah, Salt Lake City, Utah 84112

(Received 26 April 2007; accepted 15 May 2007; published online 5 July 2007)

The authors report the first gas-phase spectroscopic investigation of diatomic vanadium molybdenum (VMo). The molecules were produced by laser ablation of a VMo alloy disk and cooled in a helium supersonic expansion. The jet-cooled VMo molecules were studied using resonant two-photon ionization spectroscopy. The ground state has been demonstrated to be of ${}^2\Delta_{5/2}$ symmetry, deriving from the $d\sigma^2d\pi^4d\delta^3s\sigma^2$ electronic configuration. Rotational analysis has established the ground state bond length and rotational constant as $r_0''=1.876\,57(23)$ Å and $B_0''=0.142\,861(35)$ cm⁻¹, respectively, for ${}^{51}\text{V}{}^{98}\text{Mo}$ (1 σ error limits). Transitions to states with $\Omega'=2.5$, $\Omega'=3.5$, and $\Omega'=1.5$ have been recorded and rotationally analyzed. A band system originating at 15 091 cm⁻¹ has been found to exhibit a vibrational progression with $\omega_e'=752.7$ cm⁻¹, $\omega_e'x_e'=12.8$ cm⁻¹, and $r_0'=1.90$ Å for ${}^{51}\text{V}{}^{98}\text{Mo}$. The measured bond lengths (r_0) of V₂, VNb, Nb₂, Cr₂, CrMo, Mo₂, VCr, NbCr, and VMo have been used to derive multiple bonding radii for these elements of $r(\text{V})=0.8919$ Å, $r(\text{Nb})=1.0424$ Å, $r(\text{Cr})=0.8440$ Å, and $r(\text{Mo})=0.9725$ Å. These values reproduce the bond lengths of all nine diatomics to an accuracy of ± 0.012 Å or better. © 2007 American Institute of Physics. [DOI: 10.1063/1.2747617]

I. INTRODUCTION

Spectroscopic studies of diatomic transition metals from the center of the Periodic Table, such as V₂,¹ Nb₂,² Cr₂,^{3,4} Mo₂,⁵ VNb,⁶ VCr,⁷ NbCr,⁷ CrMo,⁸ and NbMo,⁹ have provided a wealth of information relevant to the electronic structure and chemical bonding in these molecules. It has been demonstrated, both experimentally and theoretically,^{10,11} that these molecules possess *d-d* multiple bonds, in contrast to the late transition metal diatomics Ni₂,¹² Cu₂,¹³ NiCu,¹⁴ NiAu,¹⁵ NiPd,¹⁶ NiPt,¹⁷ CuAg,¹⁸ and CuAu,¹⁹ where *s* bonding dominates. In the metals from the central portion of the Periodic Table, the *d* orbitals are large enough to participate in the bonding; in contrast, the differential contraction of the *d* orbitals relative to the valence *s* orbital favors a chemical bond that is completely dominated by the *s* orbitals in the late transition metal dimers. The multiple bonding between *d* orbitals is also diminished in the late transition metal dimers because the antibonding *d*-based orbitals are being filled. Thus, the late transition metal dimers are best described as having a two-electron σ bond. The decreasing importance of *d-d* bonding as one moves to the right in the Periodic Table is evident from the steady increase in the bond length as one moves from Cr₂ to Cu₂.^{3,20} In this article, we report rotationally resolved investigations of another mixed transition metal diatomic from the center of the Periodic Table, the 11 valence electron Groups V-VI mixed diatomic, VMo.

This paper reports the first gas-phase spectroscopic study of diatomic VMo. Our results provide an experimental verification of the active *d*-orbital participation from the measured bond lengths and electronic symmetry of the ground and excited states of VMo. The experimental methods that are used are described in Sec. II, while Sec. III provides an

analysis of the vibronic and rotationally resolved spectra. A discussion of the results and a comparison of the ground state of VMo to the previously known isovalent species VCr and NbCr are presented in Sec. IV. Section V then concludes the paper with a summary of the most important results.

II. EXPERIMENT

In the present study, the production of the diatomic VMo species was accomplished by laser ablation [Nd:YAG (yttrium aluminum garnet), 355 nm, and 12 mJ/pulse] of a 4:1 molar ratio VMo alloy disk followed by supersonic expansion in helium carrier gas (160 psi). The jet-cooled molecular beam was roughly collimated by a 1 cm skimmer before entering the ionization region of a reflectron time-of-flight mass spectrometer (TOFMS).²¹ In this region the molecular beam was first probed with a tunable dye laser pumped by the second or third harmonic of a Nd:YAG laser, and any excited states produced were then one-photon ionized by an excimer laser operating on a KrF gas mixture (248 nm and 5.00 eV). The ions were mass separated in the TOFMS and detected using a microchannel plate detector. The optical spectra of ${}^{51}\text{V}{}^{92}\text{Mo}$ (14.8% natural abundance), ${}^{51}\text{V}{}^{94}\text{Mo}$ (9.3%), ${}^{51}\text{V}{}^{95}\text{Mo}$ (15.9%), ${}^{51}\text{V}{}^{96}\text{Mo}$ (16.7%), ${}^{51}\text{V}{}^{97}\text{Mo}$ (9.6%), ${}^{51}\text{V}{}^{98}\text{Mo}$ (24.1%), and ${}^{51}\text{V}{}^{100}\text{Mo}$ (9.6%) were collected by individually monitoring the ion signals at masses of 143, 145, 146, 147, 148, 149, and 151, respectively, as a function of the dye laser wave number.

The low resolution optical spectrum of VMo was recorded in the frequency range of 14 300–22 880 cm⁻¹. Rotationally resolved spectra of 11 prominent bands were recorded. This was accomplished by inserting an intracavity étalon into the grating cavity of the dye laser, thereby narrowing the laser linewidth to 0.04 cm⁻¹. The grating cavity was evacuated and the dye laser was pressure scanned with

^{a)}Fax: (801)-581-8433; Electronic mail: morse@chem.utah.edu

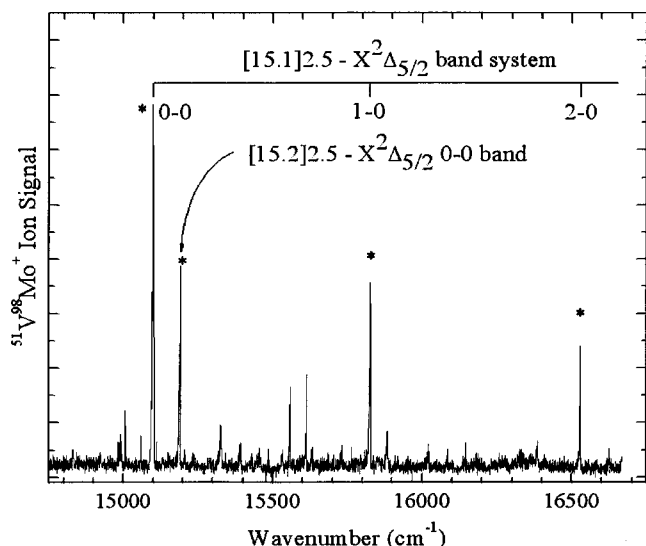


FIG. 1. Vibronically resolved spectrum of $^{51}\text{V}^{98}\text{Mo}$ in the 14 750–16 750 cm^{-1} range. Peaks labeled with an asterisk have been examined in rotationally resolved scans (~ 0.04 cm^{-1} resolution).

SF_6 . Calibration of the rotationally resolved scans was accomplished by simultaneously recording an I_2 absorption spectrum and comparing the line positions to the atlas of Gerstenkorn and Luc²² to obtain the absolute frequency. For bands to the blue of 20 000 cm^{-1} , the absorption spectrum of $^{130}\text{Te}_2$ was recorded and compared to the $^{130}\text{Te}_2$ atlas of Cariou and Luc.²³ A correction for the Doppler shift experienced by the molecules as they approached the radiation source at the beam velocity of helium, 1.77×10^5 cm/s , was included in all reported line positions.

All of the rotationally resolved transitions were found to originate from the same lower state level, which is the $v=0$ level of the $X^2\Delta_{5/2}$ ground state. Accordingly, the rotational lines from all of the assigned transitions were combined and fitted under the constraint that the B'' values for all bands are the same. This procedure significantly reduced the statistical error in the reported B'' value.

Excited state lifetimes were measured by varying the delay between the excitation and ionization lasers and recording the ion signal as a function of this delay. The exponential decay was then fitted to extract the excited state lifetime using the Marquardt nonlinear least-squares algorithm.²⁴

III. RESULTS

A. Vibronic spectrum of $^{51}\text{V}^{98}\text{Mo}$

A low resolution (~ 0.15 cm^{-1}) resonant two-photon ionization spectrum of diatomic VMo was recorded in the 14 500–22 500 cm^{-1} region. Figure 1 presents the vibronic spectrum of the most abundant isotopic species, $^{51}\text{V}^{98}\text{Mo}$, in the 14 750–16 750 cm^{-1} region, scanned using LDS 698 and DCM dyes. Bands that have been rotationally resolved are labeled with asterisks (*). The vibronic spectrum of VMo in this region reveals an intense vibrational progression corresponding to the 0-0, 1-0, and 2-0 bands of the $[15.1]2.5 \leftarrow X^2\Delta_{5/2}$ system. A strong feature displaced by 90 cm^{-1} to the blue of the 0-0 band of the main progression corresponds

to the origin band of another excited state, designated as the $[15.2]2.5$ state. The low resolution spectrum also displays many weak features which have not been rotationally resolved and are not assigned. The determination of the vibrational numbering of the $[15.1]2.5 \leftarrow X^2\Delta_{5/2}$ band system has been aided by the isotope shifts, which increase substantially as one moves from the 0-0 band, to the 1-0 band, and finally to the 2-0 band. In the lightest isotope $^{51}\text{V}^{92}\text{Mo}$, the three bands corresponding to the main progression are accompanied by weaker features, not observed in the remaining isotopes. These features probably correspond to transitions to an otherwise spin forbidden state that gain intensity by spin-orbit mixing with the $[15.1]2.5$ state, thereby becoming partially allowed. In the heavier isotopes the dark state presumably lies too far away from the $[15.1]2.5$ state to allow significant mixing, so the extra transitions are not observed.

As listed in Table I, which presents results from rotationally resolved investigations and lifetime measurements, the two electronically excited $\Omega'=2.5$ states, with T_0 values of 15 091.5 and 15 181.9 cm^{-1} in $^{51}\text{V}^{98}\text{Mo}$, exhibit similar upper state lifetimes, in the range of 3–6 μs . These lifetimes are typical of the excited state lifetimes for electronically allowed excitations in diatomic transition metals, provided that charge transfer transitions are not involved. A vibrational fit of the $v'-0$ bands of the $[15.1]2.5 \leftarrow X^2\Delta_{5/2}$ system provides the upper state vibrational frequency and anharmonicity values of $\omega'_e=752.7$ cm^{-1} and $\omega'_e x'_e=12.8$ cm^{-1} , respectively. As far as we are aware, this is the largest vibrational frequency ever measured for a transition metal diatomic, even exceeding the values of $\Delta G_{1/2}$ found for the excited $^3\Pi_u$ state of V_2 (639.7 cm^{-1}),¹ the first excited $^2\Sigma^+$ state of VCr (688 \pm 15 cm^{-1}),²⁵ or for the excited $^3\Sigma^+$ state of VMn (680 \pm 15 cm^{-1}).²⁶ The vibrational constants for this band system are compromised to some degree by perturbations, which shift the positions of the vibrational levels and also disrupt the isotopic shifts so that the band origins fail to follow the expected nearly linear dependence on $\mu^{-1/2}$, particularly in the 0-0 band. Because we only observe the $v'=0, 1$, and 2 levels, these levels are uniquely fitted by the three parameters T_0 , ω'_e , and $\omega'_e x'_e$, and no estimate of the error in these parameters is possible. Perturbations are also evident in the rotationally resolved spectra, especially for the 0-0 band, where the rotational constants of the various isotopomers clearly fail to follow the expected μ^{-1} dependence. Likewise, the B'_v rotational constants measured from the 0-0, 1-0, and 2-0 bands of the $^{51}\text{V}^{98}\text{Mo}$ isotopomer also fail to follow the expected behavior of $B'_v=B_e-\alpha_e(v+1/2)$. Strong perturbations are found in nearly all of the excited states that have been rotationally resolved, as demonstrated by serious deviations from the expected μ^{-1} dependence of the rotational constant on the reduced mass. In fact, the only states that we have examined that are relatively free of perturbations are the ground state and the upper levels of the 15 182 and 20 194 cm^{-1} bands.

The energy region from 17 500 to 22 500 cm^{-1} was scanned using Coumarin 540A, 500, 480, 460, and 440 dyes. The vibronic spectrum of the $^{51}\text{V}^{98}\text{Mo}$ isotopic modification is displayed in Fig. 2, with rotationally resolved features again indicated by asterisks. The only band within this region

TABLE I. Parameters from rotationally resolved scans for VMO.

Band	Parameter	$^{51}\text{V}^{92}\text{Mo}$	$^{51}\text{V}^{94}\text{Mo}$	$^{51}\text{V}^{95}\text{Mo}$	$^{51}\text{V}^{96}\text{Mo}$	$^{51}\text{V}^{97}\text{Mo}$	$^{51}\text{V}^{98}\text{Mo}$	$^{51}\text{V}^{100}\text{Mo}$	τ (μs)
[15.1]2.5 \leftarrow X $^2\Delta_{S/2}$ 0-0 band	ν_0	15 090.4131(40)	15 093.4882(46)	15 092.4879(47)	15 092.0179(55)	15 091.7205(39)	15 091.5300(30)	15 091.2503(26)	3.10(3)
	B'	0.137 559(76)	0.137 715(72)	0.138 267(69)	0.140 045(95)	0.139 333(50)	0.138 856(39)	0.137 974(39)	
	r'	1.933 64(53)	1.925 19(50)	1.917 78(48)	1.902 10(65)	1.903 53(34)	1.903 44(27)	1.902 96(27)	
[15.2]2.5 \leftarrow X $^2\Delta_{S/2}$ 0-0 band	ν_0	15 185.7399(24)	15 184.3712(33)	15 183.7382(31)	15 183.0470(23)	15 182.5425(45)	15 181.9522(25)	15 180.7433(51)	5.25(32)
	B'	0.138 057(62)	0.136 882(83)	0.136 433(71)	0.136 000(81)	0.135 279(54)	0.134 725(52)	0.133 440(56)	
	r'	1.930 15(43)	1.931 04(59)	1.930 63(50)	1.930 18(58)	1.931 84(39)	1.932 40(37)	1.935 02(41)	
[15.1]2.5 \leftarrow X $^2\Delta_{S/2}$ 1-0 band	ν_0	15 836.7251(55)	15 828.3916(35)	15 825.4780(40)	15 822.9885(26)	15 820.7428(45)	15 818.7208(53)	15 814.8752(25)	5.61(24)
	B'	0.132 898(50)	0.136 639(51)	0.137 345(33)	0.137 480(38)	0.137 105(62)	0.137 140(32)	0.136 519(61)	
	r'	1.967 25(37)	1.932 76(36)	1.924 21(23)	1.919 76(26)	1.918 94(43)	1.915 31(22)	1.913 07(43)	
[15.1]2.5 \leftarrow X $^2\Delta_{S/2}$ 2-0 band	ν_0	16 543.5 ^a	16 533.9 ^a	16 530.7 ^a	16 526.9 ^a	16 523.5 ^a	16 520.3692(28)	16 513.8 ^a	
	B'						0.130 468(106)		
	r'						1.963 68(80)		
18 691 $\Omega'=3.5\leftarrow$ X $^2\Delta_{S/2}$	ν_0	18 692.2460(31)						18.691.0466(36)	
	B'	0.155 013(37)						0.149 451(37)	
	r'	1.821 53(22)						1.828 43(23)	
18 700 $\Omega'=2.5\leftarrow$ X $^2\Delta_{S/2}$	ν_0	18 706.5946(40)						18 686.2230(42)	
	B'	0.136 110(86)						0.137 047(75)	
	r'	1.943 90(61)						1.909 38(52)	
18 770 $\Omega'=2.5\leftarrow$ X $^2\Delta_{S/2}$	ν_0	18 771.7170(27)	18 771.5320(41)	18 770.9840(27)		18 769.9706(41)	18 768.2794(46)	18 772.5188(41)	
	B'	0.151 834(63)	0.149 904(51)	0.150 188(37)		0.143 410(95)	0.133 740(119)	0.146 210(55)	
	r'	1.840 50(38)	1.845 26(31)	1.840 097		1.876 28(62)	1.939 51(86)	1.848 58(35)	
19 320 $\Omega'=2.5\leftarrow$ X $^2\Delta_{S/2}$	ν_0	19 322.9003(52)		19 319.8675(36)	19 318.9509(44)		19 317.0564(52)	19 316.2058(68)	
	B'	0.146 262(109)		0.147 087(68)	0.146 137(43)		0.144 848(66)	0.141 055(97)	
	r'	1.875 23(70)		1.859 39(43)	1.862 03(27)		1.863 66(43)	1.882 06(65)	
20 116 $\Omega'=2.5\leftarrow$ X $^2\Delta_{S/2}$	ν_0	20 116.5881(69)	20 116.8448(33)		20 117.4855(68)	20 116.7656(31)			
	B'	0.140 203(148)	0.142 396(147)		0.139 204(64)	0.141 948(195)			
	r'	1.915 32(101)	1.893 29(98)		1.907 84(44)	1.885 917			
[20.19]3.5 \leftarrow X $^2\Delta_{S/2}$ 0-0 band	ν_0		20 194.2150(20)	20 194.0629(28)	20 193.9034(33)	20 193.7354(28)	20 193.5256(28)	20 193.0134(29)	
	B'		0.147 209(42)	0.146 693(56)	0.146 212(39)	0.145 497(54)	0.145 037(18)	0.143 713(59)	
	r'		1.862 08(27)	1.861 89(36)	1.861 55(25)	1.862 77(35)	1.862 44(12)	1.864 57(38)	
20 225 $\Omega'=3.5\leftarrow$ X $^2\Delta_{S/2}$	ν_0		20 232.8808(49)				20 223.0665(26)	20 218.4820(52)	
	B'		0.151 620(59)				0.147 643(20)	0.145 711(58)	
	r'		1.834 79(36)				1.845 93(12)	1.851 75(37)	
21 070 $\Omega'=1.5\leftarrow$ X $^2\Delta_{S/2}$	ν_0					21 072.6433(45)	21 070.5426(48)		
	B'					0.132 107(75)	0.130 898(100)		
	r'					1.954 90(56)	1.960 45(75)		
X $^2\Delta_{S/2}$ parameters	B''	0.146 035(50)	0.144 858(44)	0.144 365(41)	0.143 915(53)	0.143 286(44)	0.142 861(35)	0.141 852(49)	
	r''	1.876 68(32)	1.884 29(29)	1.887 51(27)	1.876 35(35)	1.877 09(29)	1.876 57(23)	1.876 76(32)	

^aMeasured in low resolution, likely error is ± 0.5 cm $^{-1}$.

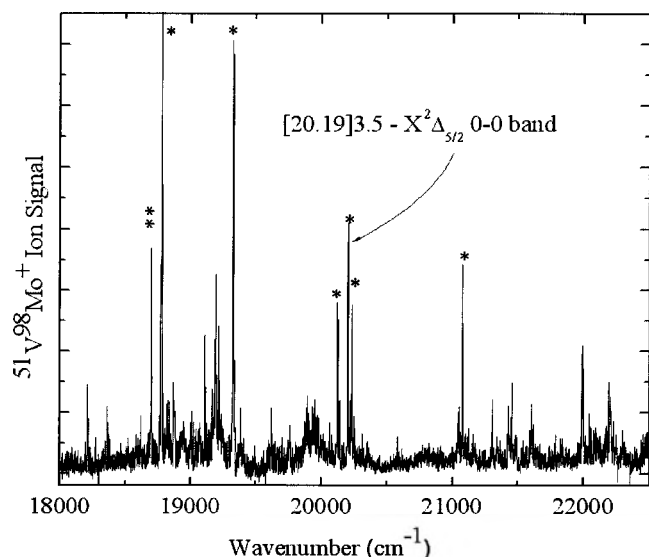


FIG. 2. Vibronically resolved spectrum of $^{51}\text{V}^{98}\text{Mo}$, covering the 18 000–22 500 cm^{-1} range. Peaks labeled with an asterisk have been examined in rotationally resolved scans.

that we assign to a specific band system is the feature near 20 194 cm^{-1} , which is free of major perturbations. Based on the small isotope shift observed, this is assigned as the 0-0 band of the $[20.19]3.5 \leftarrow X^2\Delta_{5/2}$ system. Other bands that were rotationally resolved in this region include three bands found near 18 768, 19 317, and 20 116 cm^{-1} , which have $\Omega'=2.5$, and two bands near 18 691 and 20 223 cm^{-1} , which have $\Omega'=3.5$. The upper state of a weak transition near 21 071 cm^{-1} has $\Omega'=1.5$.

The $[18.69]3.5$ and $[18.77]2.5$ vibronic levels are perturbed by nearby $\Omega=2.5$ excited states. The Ω value of the perturber could be determined by analyzing the rotational structure observed in certain isotopes, for which the perturber was well separated from other transitions. Based on the weak intensity of the perturber state, it is very likely that transitions to the perturber are electronically or Franck-Condon forbidden, gaining oscillator strength by mixing with the nearby allowed transitions. Most of the transitions that were rotationally resolved exhibit small but often erratic isotope shifts, with the exception of the bands near 20 223 and 21 071 cm^{-1} , for which large isotope shifts were observed. The transitions near 18 768, 19 317, and 20 116 cm^{-1} show especially small isotope shifts, suggesting that these transitions likely correspond to origin bands. Despite the perturbations that are evident in the spectra of VMo, the rotational analysis of a total of 12 bands described below allowed precise values of the rotational constant and bond length to be determined for the $X^2\Delta_{5/2}$ ground state of VMo.

B. Rotationally resolved spectra of VMo

1. The $[15.1]2.5 \leftarrow X^2\Delta_{5/2}$ band system of VMo

Figure 3 displays the rotationally resolved spectra recorded for the 0-0 band of the $[15.1]2.5 \leftarrow X^2\Delta_{5/2}$ system of $^{51}\text{V}^{98}\text{Mo}$, the most abundant isotopomer, along with the other six isotopomers. It is evident from the figure that the isotope shift increases with mass, the lighter isotopes appearing at higher wave numbers. The lightest isotopomer,

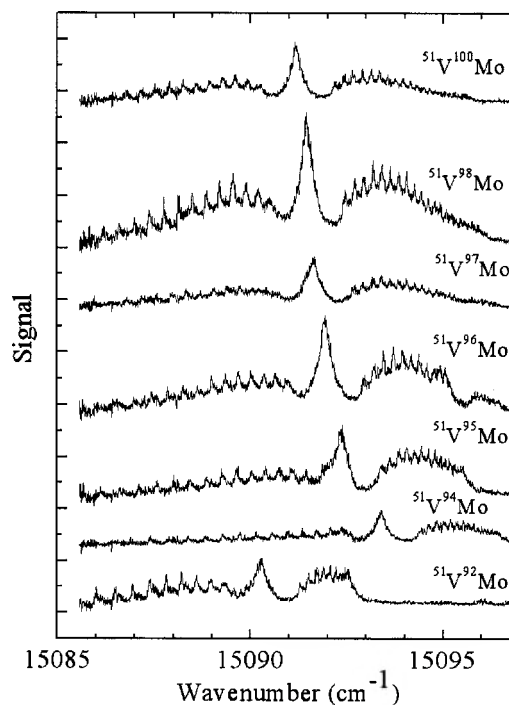


FIG. 3. Rotationally resolved spectra ($\sim 0.04 \text{ cm}^{-1}$ resolution) of the 0-0 band of the $[15.1]2.5 \leftarrow X^2\Delta_{5/2}$ band system, for all isotopes of VMo.

$^{51}\text{V}^{92}\text{Mo}$, however, is perturbed by a nearby electronic state, and is shifted to the red of the heavier isotopomers, contrary to the trend. In addition, it is obvious that the R branch forms a bandhead at much lower values of J in $^{51}\text{V}^{92}\text{Mo}$ than in the other isotopic modifications. For the heavier isotopomers, the rotationally resolved spectra display nearly symmetric P and R branches that fan out from a strong unresolved Q branch at the center of the band. The distribution of intensity among the branches allows the transition to be identified as a $\Delta\Omega=0$ band, according to the Hönl-London intensity formulas.²⁷ The R lines become more closely spaced toward higher J , while the P lines move farther apart at higher J , indicating that the bandhead lies in the R branch, corresponding to an increase in the bond length upon electronic excitation. This expectation is confirmed by the detailed rotational fitting of the band. The observation of $R(2.5)$ and $P(3.5)$ as the first lines in the R and P branches, respectively, identifies the band as an $\Omega'=2.5 \leftarrow \Omega''=2.5$ transition. Similar results are obtained for the 1-0 band of this system, near 15 819 cm^{-1} , and for the 2-0 band at 16 520 cm^{-1} .

Line positions for these and all other rotationally resolved bands for all of the interpretable isotopomers of VMo have been deposited with the Electronic Physics Auxillary Publication Service (EPAPS) of the American Institute of Physics²⁸ and are also available from one of the authors (M.D.M). The electronic document also contains spectra for all of the rotationally resolved bands, similar to that presented in Fig. 3. The line positions were fit to the following standard formula:

$$\nu = \nu_0 + B'J'(J'+1) - B''J''(J''+1), \quad (3.1)$$

to determine the band origins and rotational constants. Attempts to fit the B'_v values of the individual bands for $^{51}\text{V}^{98}\text{Mo}$ to the expression

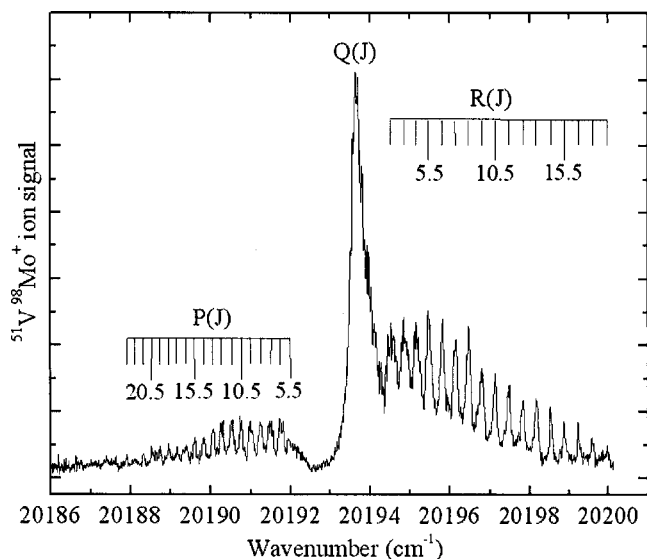


FIG. 4. Rotationally resolved scan over the $[20.19]3.5 \leftarrow X^2\Delta_{5/2}$ band of $^{51}\text{V}^{98}\text{Mo}$.

$$B'_v = B'_e - \alpha'_e(v' + 1/2) \quad (3.2)$$

failed to provide a good fit, presumably due to perturbations affecting the rotational structure, especially in the $v'=0$ level.

2. The remaining $\Omega'=2.5 \leftarrow X^2\Delta_{5/2}$ transitions

Among the other rotationally resolved bands, there appear four bands with an $\Omega'=2.5$ upper state that are observed near 15 182, 18 768, 19 317, and 20 116 cm^{-1} . The rotationally resolved spectra in all of these bands are characterized by a generally unresolved central Q branch and P and R branches of nearly equal intensities. The assignment of the first rotational lines as $P(3.5)$ and $R(2.5)$ confirms that these bands are $\Omega'=2.5 \leftarrow \Omega''=2.5$ excitations. The rotationally resolved spectra of the 15 182 and 20 116 cm^{-1} bands display a bandhead in the R branch at high J , indicating an increase in the bond length upon electronic excitation. This is in contrast to the P bandheads observed in the 18 768 and 19 317 cm^{-1} bands, which suggest a decrease in the bond length upon excitation. The fitted values of the band origin (ν_0), the rotational constant (B'), and the bond length (r') calculated from B' are again provided in Table I. Owing to perturbations in the upper states, it is often found that the r' values obtained by simple inversion of the B' values vary quite significantly with isotopic composition for a given band. Such a strong variation indicates that the r' values are not physically meaningful. They are provided simply to allow the reader to assess the magnitude of the perturbations that afflict a particular band.

3. The $\Omega'=3.5 \leftarrow X^2\Delta_{5/2}$ transitions

Transitions with an $\Omega'=3.5$ upper state are found at 18 691, 20 194, and 20 223 cm^{-1} . Figure 4 displays a rotationally resolved scan over the 20 194 cm^{-1} band of $^{51}\text{V}^{98}\text{Mo}$. The band possesses an unresolved Q branch of overlapping lines and an R branch that is much more intense

than the P branch. This intensity pattern is a characteristic of a $\Delta\Omega=+1$ transition. The large gap between the Q and P branches indicates that several of the low- J P lines are missing. For this particular band, the rotational lines are broadened quite significantly, and the broadening becomes most severe in the low- J lines of the R and P branches. This is a classic signature of unresolved hyperfine splitting in a Hund's case (a_β) molecule, which in this case fragments the first P lines into a sea of unresolved hyperlines. For $^{51}\text{V}^{98}\text{Mo}$, the hyperfine splitting is due to the interaction between an unpaired electron and the nuclear spin of ^{51}V ($I=7/2$) (^{98}Mo has $I=0$). This interaction splits each rotational level with $J \geq 3.5$ into eight hyperlevels, which are unresolved at our laser linewidth of $\sim 0.04 \text{ cm}^{-1}$.

The bandhead appears in the P branch at high J , indicating a modest decrease in the bond length that accompanies the electronic excitation, a result that is confirmed by the detailed analysis and r' values. For this particular band there is little evidence of significant perturbations, so the r' value probably has real physical meaning. Further, the small variation in the band origin with reduced mass, which is a nearly linear function of $\mu^{-1/2}$, indicates that the 20 194 cm^{-1} transition is unperturbed and is vibrationally a 0-0 band. The small change in the bond length explains why the 1-0 band is not prominent in the spectrum displayed in Fig. 2. Based on all of these observations, we feel justified in assigning this feature as the 0-0 band of the $[20.19]3.5 \leftarrow X^2\Delta_{5/2}$ band system.

The rotational structure and branch intensities of the bands at 18 691 and 20 223 cm^{-1} are similar to that displayed in Fig. 3, although neither of these bands display hyperfine broadening to the same extent. The assignment of the first lines in the 18 691 and 20 223 bands as $R(2.5)$ and $P(4.5)$ demonstrates that they are also $\Omega'=3.5 \leftarrow \Omega''=2.5$ excitations, as is also evident from the observed pattern of branch intensities.

In very close proximity to the 18 691 cm^{-1} $\Omega'=3.5 \leftarrow \Omega''=2.5$ band lies a much weaker perturbing state which exhibits a strong isotope shift. In the lightest isotope, $^{51}\text{V}^{92}\text{Mo}$, the perturbing state lies approximately 14 cm^{-1} to the red of the 18 691 cm^{-1} band, while in the heaviest isotope $^{51}\text{V}^{100}\text{Mo}$ it lies 5 cm^{-1} to the red. The perturber state shifts through the 18 691 cm^{-1} feature as the reduced mass varies, causing the rotational structure to be hopelessly complicated for all except the heaviest and lightest isotopomers. For $^{51}\text{V}^{92}\text{Mo}$ and $^{51}\text{V}^{100}\text{Mo}$, however, both states could be nicely resolved and analyzed, a result that permitted a definitive assignment of the upper states as $\Omega'=3.5$ for the strong transition and $\Omega'=2.5$ for the weaker transition.

4. The $[21.07]1.5 \leftarrow X^2\Delta_{5/2}$ band of VMO

Figure 5 displays the rotationally resolved scan over the 21 071 cm^{-1} band of $^{51}\text{V}^{98}\text{Mo}$. The band is characterized by a strong Q branch that is degraded to the red, an intense P branch, and a much weaker R branch, characteristic of a $\Delta\Omega=-1$ transition. The spectrum also shows a very rapid bandhead formation in the R branch, indicating a significant increase in the excited state bond length. The presence of

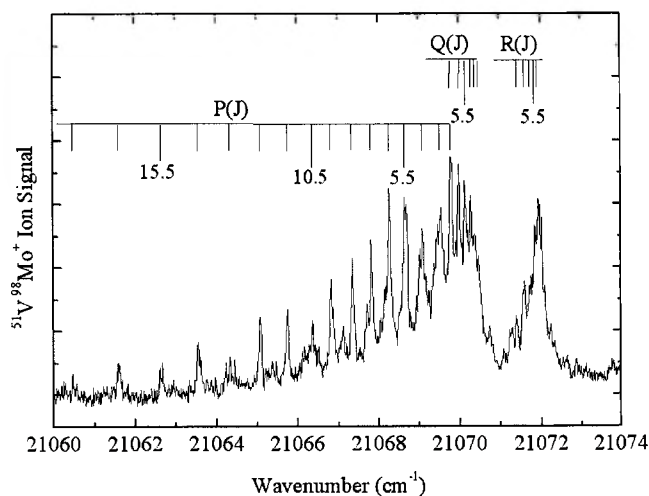


FIG. 5. Rotationally resolved scan over the $21070\text{ cm}^{-1}\ \Omega' = 1.5 \leftarrow X^2\Delta_{5/2}$ band of $^{51}\text{V}^{98}\text{Mo}$.

$R(2.5)$, $Q(2.5)$, and $P(2.5)$ identifies the transition as an $\Omega' = 1.5 \leftarrow \Omega'' = 2.5$ excitation. A least-squares fit of the observed rotational lines to Eq. (3.1) provides the excited state rotational constant $B' = 0.13090(10)\text{ cm}^{-1}$ for $^{51}\text{V}^{98}\text{Mo}$. When inverted, this provides $r' = 1.9604(8)\text{ \AA}$. The existence of significant perturbations in many of the isotopomers for this band, however, suggests that this value of r' is not physically significant.

IV. DISCUSSION

In the present investigation, all of the rotationally resolved bands arise from an $\Omega'' = 2.5$ lower state. Given the likely molecular orbital configurations, this can only arise from the valence orbital configuration $d\sigma^2d\pi^4d\delta^3s\sigma^2$, giving a $^2\Delta_{5/2}$ ground state. The alternative possibilities of a $d\sigma^2d\pi^4d\delta^4s\sigma^1$, $^2\Sigma^+(\Omega'' = 0.5)$ or a $d\sigma^2d\pi^4d\delta^3s\sigma^2s\sigma^*$, $^4\Sigma^-(\Omega'' = 0.5\text{ or }1.5)$ ground state are inconsistent with the measured spectra. Thus, diatomic VMo has the same ground configuration and term as the isovalent VCr and NbCr molecules.⁷ In these molecules the $^2\Delta_{5/2}$ ground term correlates diabatically with the combination of a $d^4s^1(^6D)$ Group V atom and a $d^5s^1(^7S)$ Group VI atom. The 7S_3 level is the ground state for the Cr and Mo (Group VI) atoms, while the $^6D_{1/2}$ level for the V (Group V) atom lies 2112.32 cm^{-1} above the $3d^34s^2(^4F_{3/2})$ ground level.²⁹ As a result about 2100 cm^{-1} of the promotion energy is required to prepare the vanadium atom for bonding in the VCr and VMo molecules.

Like VCr and NbCr, the $^2\Delta_{5/2}$ ground state of VMo derives from a $d\sigma^2d\pi^4d\delta^3s\sigma^2$ configuration, giving a nominal bond order of 5.5. The ground state bond lengths of the related molecules CrMo,⁸ VNb,³⁰ VCr,⁷ and NbCr⁷ have been shown to be nearly equal to the averages of their homonuclear counterparts. To obtain the best estimate of the VMo ground state bond length, the measured value of the effective rotational constant for the $X^2\Delta_{5/2}$ ground state, $B''_0(5/2)$, was converted to the true B''_0 value by taking into account the effects of the spin-uncoupling operator via the formula:²⁷

TABLE II. Multiple bonding radii for V, Cr, Nb, and Mo.

	V	Cr	Nb	Mo
	0.8919 \AA	0.8440 \AA	1.0424 \AA	0.9725 \AA
Molecule	Measured r_0 (\AA)	Reference	Fitted or predicted r_0 (\AA)	Fitted-measured (\AA)
V ₂	1.7758	33	1.7837	0.0079
VNb	1.9433	30	1.9342	-0.0091
Nb ₂	2.0785	2	2.0847	0.0062
VCr	1.7260	7	1.7359	0.0099
VMo	1.8766	this work	1.8644	-0.0122
NbCr	1.8939	7	1.8864	-0.0075
NbMo	Unknown		2.0149	
Cr ₂	1.6858	35	1.6881	0.0023
CrMo	1.8231	8	1.8166	-0.0065
Mo ₂	1.940	5	1.9451	0.0051

$$B_{\text{eff}}(\Omega) = B_{\text{true}} \left(1 + \frac{2B_{\text{true}}\Sigma}{A\Lambda} \right). \quad (4.1)$$

For the $d\delta^3$, $^2\Delta$ ground term of VMo, the spin-orbit parameter A , may be estimated using the semiempirical method of Ishiguro and Kobori,³¹ providing

$$A = -[\zeta_V(3d) + \zeta_{\text{Mo}}(4d)]/2, \quad (4.2)$$

where the atomic spin-orbit constants $\zeta_V(3d) = 177\text{ cm}^{-1}$ and $\zeta_{\text{Mo}}(4d) = 677\text{ cm}^{-1}$ are taken from the compilation of Lefebvre-Brion and Field.³² After combining the data for all of the VMo isotopomers and correcting for the effects of spin uncoupling, our best estimate of the VMo ground state bond length r''_0 is $1.87662(10)\text{ \AA}$, which is very close to the average (1.858 \AA) of the spin-uncoupling corrected bond lengths of V₂ ($r''_0 = 1.776\text{ \AA}$) (Ref. 33) and Mo₂ ($r''_0 = 1.940\text{ \AA}$).⁵ The short ground state bond length indicates extensive d orbital contributions to the chemical bonding, as has been previously observed in V₂ and Mo₂.

Using the measured ground state bond lengths (r''_0 , corrected for spin uncoupling effects) of V₂, VNb, Nb₂, Cr₂, CrMo, Mo₂, VCr, NbCr, and now VMo, the previously reported⁷ multiple bonding radii for V, Cr, Nb, and Mo may be revised. This is accomplished by assuming that the r_0 bond lengths of the molecules are the sum of the multiple bonding radii of the elements, which are then derived from the r_0 values by a least-squares fit. The results are provided in Table II. These values allow the bond length of NbMo to be predicted as 2.015 \AA . We are currently testing this prediction by rotationally resolved studies on NbMo, which will be presented in a separate publication.

The high density of electronic states that we observe in the VMo molecule is not at all unexpected. Even if we restrict ourselves to electric dipole-allowed transitions from the ground state, the $\delta^* \leftarrow \delta$ electronic excitation leads to two excited $^2\Delta$ terms and one $^2\Phi$ term. Similarly, the $s\sigma^* \leftarrow s\sigma$ electronic excitation generates two excited $^2\Delta$ terms. The $\delta \leftarrow \pi$ excitation generates a $^2\Pi$ term. All of these electronically allowed transitions can lend oscillator strength to spin-forbidden transitions through spin-orbit coupling, thereby making many forbidden transitions partially allowed. From the separated atom point of view, the ground $^2\Delta$ term corre-

lates to an electronically excited V atom in its $3d^44s^1$, 6D state interacting with a ground state Mo atom ($4d^55s^1$, 7S). This limit, which lies approximately 2100 cm^{-1} above ground state atoms, also leads to a ${}^2\Pi$ term that can be reached by allowed electric dipole transitions from the ${}^2\Delta$ ground term. Nearly $11\,000\text{ cm}^{-1}$ above ground state atoms, however, lie the $V(3d^34s^2, {}^4F)+\text{Mo}(4d^55s^1, {}^5S)$ and $V(3d^34s^2, {}^4F)+\text{Mo}(4d^45s^2, {}^5D)$ limits, which together generate four ${}^2\Phi$ terms, five ${}^2\Delta$ terms, and six ${}^2\Pi$ terms. Thus, there are a large number of allowed transitions in the VMO molecule, and many more transitions that become accessible when spin-orbit mixing is considered.

The $[15.1]2.5$ and $[15.2]2.5$ excited states clearly derive their oscillator strength from an excited ${}^2\Delta$ term, since there is no other possibility that can provide oscillator strength for an $\Omega'=2.5 \leftarrow {}^2\Delta_{5/2}$ transition. From a molecular orbital point of view, these transitions probably correspond to a $\delta^* \leftarrow \delta$ excitation, because the upper state lifetime is much too long for a $\sigma^* \leftarrow \sigma$ excitation. Although a $\pi^* \leftarrow \pi$ transition could also account for an $\Omega'=2.5 \leftarrow X^2\Delta_{5/2}$ transition, one would expect a large increase in the bond length for such a transition, which is not observed. In Cr_2 , CrMo , and Mo_2 , the $\sigma^* \leftarrow \sigma$ excited states fluoresce back to the ground state with lifetimes that are in the range of $15\text{--}20\text{ ns}$,^{3,8} rather than the $3\text{--}6\text{ }\mu\text{s}$ measured here. Although perturbations make it difficult to accurately know the bond lengths in the excited states, it seems that these two $\Omega'=2.5$ states have bond lengths that are about $0.03\text{--}0.06\text{ \AA}$ longer than that of the ground state. This is also consistent with a $\delta^* \leftarrow \delta$ excitation, since the $\sigma^* \leftarrow \sigma$ excitations in Cr_2 , CrMo , and Mo_2 lead to much smaller increases in bond length of 0.008 \AA or less.^{3,5,8} Finally, a $\sigma^* \leftarrow \sigma$ excitation would leave an unpaired electron in a σ orbital, and would probably lead to much greater hyperfine splitting than is observed in these two band systems, due to the Fermi contact interaction³⁴ that develops between the σ or σ^* electron (which has significant s character, and therefore penetrates to the nucleus) and the ${}^{51}\text{V}$ ($I=7/2$) nuclear spin.

The $[20.19]3.5$ state must be either a ${}^2\Phi_{7/2}$ state or must obtain its intensity by spin-orbit mixing with a ${}^2\Phi_{7/2}$ state. There is simply no other electric dipole allowed source of intensity for a transition originating in a good Hund's case (a) ${}^2\Delta_{5/2}$ state and terminating on a state with $\Omega'=3.5$. Orbital excitations that could lead to a ${}^2\Phi$ term include (1) a $\pi^* \leftarrow \sigma$ excitation, leading to a $d\sigma^2d\pi^4d\delta^3s\sigma^1d\pi^{*1}$ configuration, which produces two ${}^2\Phi$ states, (2) a $\sigma^* \leftarrow \pi$ excitation, leading to a $d\sigma^2d\pi^3d\delta^3s\sigma^2s\sigma^{*1}$ configuration, which also produces two ${}^2\Phi$ terms, (3) a $\delta^* \leftarrow \pi$ excitation, leading to a $d\sigma^2d\pi^3d\delta^3s\sigma^2d\delta^{*1}$ configuration, which also produces two ${}^2\Phi$ terms, and (4) a $\pi^* \leftarrow \delta$ transition, leading to a $d\sigma^2d\pi^4d\delta^2s\sigma^2d\pi^{*1}$ configuration, which produces one ${}^2\Phi$ term. None of these electronic excitations seem likely to decrease the bond length in this molecule (as is found in our investigation), because an electron is either removed from the strongly bonding $d\pi$ orbital or placed in the corresponding antibonding $d\pi^*$ orbital. Perhaps the most likely of the various possibilities is the $\pi^* \leftarrow \sigma$ excitation, because for this excitation the decrease in the bond length expected from occupation of the $d\pi^*$ orbital may be offset by the possibility of

favorable $s\sigma\text{-}d\sigma$ hybridization in the resulting $d\sigma^2d\pi^4d\delta^3s\sigma^1d\pi^{*1}$ configuration. By placing the molecule in a state with a singly occupied σ orbital, the hyperfine interaction in the upper state is expected to increase significantly through the Fermi contact interaction. This is found to be the case for the $[20.19]3.5 \leftarrow X^2\Delta_{5/2}$ transition, which has a more significant hyperfine broadening than most of the other bands that have been examined.

The upper state of the $[21.07]1.5 \leftarrow X^2\Delta_{5/2}$ transition must either be a ${}^2\Pi$ term or must gain its intensity by spin-orbit mixing with a ${}^2\Pi$ term. The excitations discussed in the last paragraph all generate ${}^2\Pi$ terms, in addition to the ${}^2\Phi$ terms. Altogether, these electronic excitations generate ten ${}^2\Pi$ terms. Thus, there are a large number of potential candidates for the $[21.07]1.5$ level, even without considering transitions that are made allowed by spin-orbit coupling. For this band we observe a large isotope shift, so it is not an origin band; secondly, the band shows perturbations in the upper state, preventing a meaningful measurement of the bond length. Thus, we have no basis whatever for attempting to assign a configuration to this level. There is every reason to expect extensive configuration interaction in this molecule, in any event.

V. CONCLUSION

The VMO diatomic molecule has been investigated by the resonant two-photon ionization technique. Excited states with $\Omega=1.5$, 2.5 , and 3.5 have been observed in the $14\,500\text{--}22\,500\text{ cm}^{-1}$ region. All of the transitions originate from the same $\Omega''=2.5$ level, which is the $v=0$ level of the $X^2\Delta_{5/2}$ ground state. The analysis of the rotationally resolved spectra of about a dozen bands has allowed the ground state to be characterized by $r_0''=1.876\,62(10)\text{ \AA}$, after a correction for spin-uncoupling effects between the $X^2\Delta_{5/2}$ ground level and its spin-orbit excited ${}^2\Delta_{3/2}$ level. It is suggested that the $\Omega=2.5$ excited states that are observed are predominantly $d\delta^* \leftarrow d\delta$ excitations, while the $[20.19]3.5$ state arises primarily from a $\pi^* \leftarrow \sigma$ excitation. The bond length in the ground state of VMO is very close to the average of the ground state bond lengths of the corresponding homonuclear molecules (V_2 and Mo_2), a trend that has been observed in the other Groups V-VI intermetallic dimers. Based on this observation, a set of multiple bonding radii for V, Cr, Nb, and Mo has been derived. These reproduce the measured bond lengths to an accuracy of $\pm 0.012\text{ \AA}$.

ACKNOWLEDGMENT

This material is based upon the work supported by the National Science Foundation under Grant No. CHE-0415647.

¹P. R. R. Langridge-Smith, M. D. Morse, G. P. Hansen, R. E. Smalley, and A. J. Merer, *J. Chem. Phys.* **80**, 593 (1984).

²A. M. James, P. Kowalczyk, R. Fournier, and B. Simard, *J. Chem. Phys.* **99**, 8504 (1993).

³D. L. Michalopoulos, M. E. Geusic, S. G. Hansen, D. E. Powers, and R. E. Smalley, *J. Phys. Chem.* **86**, 3914 (1982).

⁴S. M. Casey and D. G. Leopold, *J. Phys. Chem.* **97**, 816 (1993).

⁵J. B. Hopkins, P. R. R. Langridge-Smith, M. D. Morse, and R. E. Smalley, *J. Chem. Phys.* **78**, 1627 (1983).

- ⁶A. M. James, P. Kowalczyk, E. Langlois, M. D. Campbell, A. Ogawa, and B. Simard, *J. Chem. Phys.* **101**, 4485 (1994).
- ⁷S. M. Sickafoose, J. D. Langenberg, and M. D. Morse, *J. Phys. Chem. A* **104**, 3521 (2000).
- ⁸E. M. Spain, J. M. Behm, and M. D. Morse, *Chem. Phys. Lett.* **179**, 411 (1991).
- ⁹W. E. Klotzbücher and G. A. Ozin, *Inorg. Chem.* **19**, 2848 (1980).
- ¹⁰M. M. Goodgame and W. A. Goddard III, *Phys. Rev. Lett.* **48**, 135 (1982).
- ¹¹S. P. Walch, C. W. Bauschlicher, Jr., B. O. Roos, and C. J. Nelin, *Chem. Phys. Lett.* **103**, 175 (1983).
- ¹²M. D. Morse, G. P. Hansen, P. R. R. Langridge-Smith, L.-S. Zheng, M. E. Geusic, D. L. Michalopoulos, and R. E. Smalley, *J. Chem. Phys.* **80**, 5400 (1984).
- ¹³J. G. McCaffrey, R. R. Bennett, M. D. Morse, and W. H. Breckenridge, *J. Chem. Phys.* **91**, 92 (1989).
- ¹⁴Z. Fu and M. D. Morse, *J. Chem. Phys.* **90**, 3417 (1989).
- ¹⁵E. M. Spain and M. D. Morse, *J. Chem. Phys.* **97**, 4605 (1992).
- ¹⁶S. Taylor, E. M. Spain, and M. D. Morse, *J. Chem. Phys.* **92**, 2710 (1990).
- ¹⁷S. Taylor, E. M. Spain, and M. D. Morse, *J. Chem. Phys.* **92**, 2698 (1990).
- ¹⁸G. A. Bishea, N. Marak, and M. D. Morse, *J. Chem. Phys.* **95**, 5618 (1991).
- ¹⁹G. A. Bishea, J. C. Pinegar, and M. D. Morse, *J. Chem. Phys.* **95**, 5630 (1991).
- ²⁰R. S. Ram, C. N. Jarman, and P. F. Bernath, *J. Mol. Spectrosc.* **156**, 468 (1992).
- ²¹B. A. Mamyryn, V. I. Karataev, D. V. Shmikk, and V. A. Zagulin, *Zh. Eksp. Teor. Fiz.* **64**, 82 (1973).
- ²²S. Gerstenkorn and P. Luc, *Atlas du Spectre d'Absorption de la Molécule d'Iode entre 14,800–20,000 cm⁻¹* (CNRS, Paris, 1978).
- ²³J. Cariou and P. Luc, *Atlas du Spectre d'Absorption de la Molécule de Tellure entre 18,500–23,800 cm⁻¹* (CNRS, Paris, 1980).
- ²⁴P. R. Bevington, *Data Reduction and Error Analysis for the Physical Sciences* (McGraw-Hill, New York, 1969).
- ²⁵S. Alex, Ph.D. thesis, University of Minnesota, 1997.
- ²⁶T. P. Marcy, Ph.D. thesis, University of Minnesota, 1999.
- ²⁷G. Herzberg, *Molecular Spectra and Molecular Structure I. Spectra of Diatomic Molecules*, 2nd ed. (Van Nostrand Reinhold, New York, 1950).
- ²⁸See EPAPS Document No. E-JCPSA6-127-011725 for 26 pages of line positions, rotational fits, and rotationally resolved spectra. A direct link to this document may be found in the online article's HTML reference section. The document may also be reached via the EPAPS homepage (<http://www.aip.org/pubservs/epaps.html>) or from <ftp.aip.org> in the directory/epaps. See the EPAPS homepage for more information.
- ²⁹C. E. Moore, *Atomic Energy Levels*, Natl. Bur. Stand. (U.S.) Circ. No. 467 (U.S. GPO, Washington, D.C., 1971).
- ³⁰A. M. James, P. Kowalczyk, and B. Simard, *Chem. Phys. Lett.* **216**, 512 (1993).
- ³¹E. Ishiguro and M. Kobori, *J. Phys. Soc. Jpn.* **22**, 263 (1967).
- ³²H. Lefebvre-Brion and R. W. Field, *The Spectra and Dynamics of Diatomic Molecules* (Elsevier, Amsterdam, 2004).
- ³³E. M. Spain, J. M. Behm, and M. D. Morse, *J. Chem. Phys.* **96**, 2511 (1992).
- ³⁴T. M. Dunn, in *Molecular Spectroscopy: Modern Research*, edited by K. N. Rao and C. W. Mathews (Academic, New York, 1972), pp. 231–57.
- ³⁵V. E. Bondybey and J. H. English, *Chem. Phys. Lett.* **94**, 443 (1982).